Association of urban forest landscape characteristics with biomass and soil carbon stocks in Harbin City, Northeastern China

Hailiang Lv [1, 2] , Wenjie Wang [Corresp., 1, 2] , Xingyuan He [1] , Chenhui Wei [1] , Lu Xiao [1] , Bo Zhang [2] , Wei Zhou [2]

[1] Northeast Institute of Geography and Agricultural Ecology, Chinese Academy of Sciences, Changchun, The People's Republic of China

[2] Northeast Forestry University, Harbin, The People's Republic of China

Corresponding Author: Wenjie Wang
Email address: wangwenjie@iga.ac.cn

Background . Urban forests help in mitigating carbon emissions; however, their associations with landscape patterns are unclear. Understanding the associations would help us to evaluate urban forest ecological services and favor urban forest management via landscape regulations. We used Harbin, capital city of the northernmost province in China, as an example and hypothesized that the urban forests had different landscape metrics among different forest types, administrative districts, and urban–rural gradients, and these differences were closely associated with forest carbon sequestration in the biomass and soils.

Methods. We extracted the urban forest tree coverage area on the basis of 2 GF-1 remote sensing images and object-oriented based classification method. The analysis of forest landscape patterns and estimation of carbon storage were based on tree coverage data and 199 plots . We also examined the relationships between forest landscape metrics and carbon storage on the basis of forest types, administrative districts, ring roads, and history of urban settlements by using statistical methods.

Results. The small patches covering an area of less than 0.5 ha accounted for 72.6% of all patches (average patch size, 0.31 ha). The mean patch size (AREA_MN) and largest patch index (LPI) were the highest in the landscape and relaxation forest and Songbei District. The landscape shape index (LSI) and number of patches linearly decreased along rural-urban gradients ($p < 0.05$). The tree biomass carbon storage varied from less than 10 thousand tons in the urban center (first ring road region and 100-year regions) to more than 100 thousand tons in the rural regions (fourth ring road and newly urbanized regions). In the same urban–rural gradients, soil carbon storage varied from less than 5 thousand tons in the urban centers to 73–103 thousand tons in the rural regions. The association analysis indicated that the total forest area was the key factor that regulates total carbon storage in trees and soils. However, in the case of carbon density (ton ha^{-1}), AREA_MN was strongly associated with tree biomass carbon, and soil carbon density was negatively related to LSI ($p < 0.01$) and AREA_MN ($p < 0.05$), but positively related to LPI ($p < 0.05$).

Discussion. The urban forests were more fragmented in Harbin than in other provincial cities in Northeastern China, as shown by the smaller patch size, more complex patch shape, and larger patch density. The decrease in LSI along the rural-urban gradients may contribute to the forest carbon sequestrations in downtown regions, particularly underground soil carbon accumulation, and the increasing patch size may benefit tree carbon sequestration. Our findings help us to understand how forest landscape metrics are associated with carbon storage function. These findings related to urban forest design may maximize forest carbon sequestration services and facilitate in precisely estimating

the forest carbon sink.

2 Association of urban forest landscape characteristics with biomass and soil carbon stocks in
3 Harbin City, Northeastern China

5 Hailiang Lv [1,2], Wenjie Wang [1,2], Xingyuan He [1], Chenhui Wei[1], Lu Xiao[1], Bo Zhang[2], Wei
6 Zhou[2]

7 [1] Northeast Institute of Geography and Agricultural Ecology, Chinese Academy of Sciences,
8   Changchun 130102, Jilin, China;
9 [2] Northeast Forestry University, No. 26 Hexing Road, Harbin 10040, China

10 Corresponding author:
11 Wenjie wang

12 Email address: wjwang225@hotmail.com

14 **Abstract**

15 **Background.** Urban forests help in mitigating carbon emissions; however, their associations with

16 landscape patterns are unclear. Understanding the associations would help us to evaluate urban

17 forest ecological services and favor urban forest management via landscape regulations. We used

18 Harbin, capital city of the northernmost province in China, as an example and hypothesized that

19 the urban forests had different landscape metrics among different forest types, administrative

20 districts, and urban–rural gradients, and these differences were closely associated with forest

21 carbon sequestration in the biomass and soils.

22 **Methods.** We extracted the urban forest tree coverage area on the basis of 2 GF-1 remote sensing

23 images and object-oriented based classification method. The analysis of forest landscape patterns

24 and estimation of carbon storage were based on tree coverage data and 199 plots. We also

25 examined the relationships between forest landscape metrics and carbon storage on the basis of

26 forest types, administrative districts, ring roads, and history of urban settlements by using

27 statistical methods.

28 **Results.** The small patches covering an area of less than 0.5 ha accounted for 72.6% of all patches

29 (average patch size, 0.31 ha). The mean patch size (AREA_MN) and largest patch index (LPI)

30 were the highest in the landscape and relaxation forest and Songbei District. The landscape shape

31 index (LSI) and number of patches linearly decreased along rural-urban gradients ($p < 0.05$). The

32 tree biomass carbon storage varied from less than 10 thousand tons in the urban center (first ring

33 road region and 100-year regions) to more than 100 thousand tons in the rural regions (fourth ring

34 road and newly urbanized regions). In the same urban–rural gradients, soil carbon storage varied

35 from less than 5 thousand tons in the urban centers to 73–103 thousand tons in the rural regions.

36 The association analysis indicated that the total forest area was the key factor that regulates total

37 carbon storage in trees and soils. However, in the case of carbon density (ton ha^{-1}), AREA_MN

38 was strongly associated with tree biomass carbon, and soil carbon density was negatively related

39 to LSI ($p < 0.01$) and AREA_MN ($p < 0.05$), but positively related to LPI ($p < 0.05$).

40 **Discussion.** The urban forests were more fragmented in Harbin than in other provincial cities in

41 Northeastern China, as shown by the smaller patch size, more complex patch shape, and larger

42 patch density. The decrease in LSI along the rural-urban gradients may contribute to the forest

43 carbon sequestrations in downtown regions, particularly underground soil carbon accumulation,

44 and the increasing patch size may benefit tree carbon sequestration. Our findings help us to

45 understand how forest landscape metrics are associated with carbon storage function. These

46 findings related to urban forest design may maximize forest carbon sequestration services and

47 facilitate in precisely estimating the forest carbon sink.

48

Introduction

The value of urban forests in mitigating carbon emissions has received considerable interest among scientists and urban planners (Zhao et al., 2010; Setala et al., 2013) because of accelerated urbanization and ecological and environmental problems worldwide (Maruotti, 2008; Mccarthy et al., 2010; Zhao et al., 2015; Zhao & Wentz, 2016). The carbon sink function of urban forests in many cities such as Miami-Dade and Gainesville, USA (Escobedo et al., 2010); Hangzhou, China (Zhao et al., 2010); and Chuncheon, Kangleung, and Seoul, Middle Korea (Jo, 2002) have been assessed for offsetting regional carbon emissions. Even though researchers worldwide have estimated the storage and sequestration of carbon in urban forests (Liu & Li, 2012; Nowak et al., 2013, Zhang et al., 2015), less attention has been paid to the relationship between the landscape pattern and carbon storage functions in urban forests (Ren et al. 2013). In general, urban regions have limited space for urban forests, and the landscape patterns of urban forests could strongly modify forest ecological services, such as species diversity conservation (Zhang et al., 2017b) and cooling island effects (Ren et al., 2013). To date, associations between carbon sinks and landscape patterns have not been well-defined, and untangling the associations is essential to precisely evaluate ecological services of urban forests (Ren et al., 2013; Zhang et al., 2017b; Ren et al., 2018; Wang et al., 2018).

Quantification of forest landscape metrics is useful for understanding the structure and configuration of the urban forest landscape (Uuemaa et al., 2013). Possible indices include area-related parameters, such as the total area for green infrastructure (TA), number of forest patches (NP), and mean patch size (AREA_MN); forest shape features, such as perimeters of patch and perimeter-area ratio (PARA); patch aggregation features, such as landscape shape index (LSI), largest patch index (LPI), and distance between patches (Liu et al., 2009; Gounaridis et al., 2014). These indices yield a lot of information and can be quantified easily by using ArcGIS and Fragstats software; they have been used as indicators in many studies on land use changes, habitat alterations, and landscape regulating functions under both urban and natural conditions (Uuemaa et al., 2013; Ren et al., 2013; Zhang et al., 2017b). Associations between urbanization intensity

76 (urban–rural gradients) and ecological services, such as carbon storage capacity, have been used

77 to understand urbanization and green infrastructure service interactions (Zhan et al., 2015; Lv et

78 al., 2016) without considering forest landscape patterns. Clarification of the relationships between

79 urban forest landscape characteristics and carbon storage may be helpful in understanding how

80 urbanization affects carbon storage in trees and soils and finding possible indicators for evaluations

81 of urban forest carbon sink functions; the possible parameters include urbanization intensity,

82 landscape metrics, and tree size and forest community attributes, etc. (Wang et al., 2005; Wang et

83 al., 2011; Zhang et al., 2017b).

84   Currently, China is in a period of rapid urbanization, and there is a general hope for good

85 environmental security from urban green vegetation, such as forests (Mu et al., 2004; Wang, 2009;

86 Liang et al., 2014; He et al., 2017; Zheng et al., 2017; Wang et al., 2018). In China, the urban

87 forests can easily be classified into different types on the basis of their location and functions, such

88 as roadside forest distributed on both sides of roads; affiliation forest in different units of

89 universities, schools, and institutes; landscape and relaxation forest in gardens and parks; and

90 ecological public welfare forest for the prevention of soil erosion, floods, etc. (He et al., 2004).

91 The division of different administrative districts in the same city facilitates possible management

92 by public and private units (Liu et al., 2007), including urban vegetation. Moreover, ring-road

93 development and the history of urban settlements indicating urban–rural gradients are typical ways

94 for understanding the urbanization effects (Xiao et al., 2016a). Studies that combine forest types,

95 administrative districts, and urban–rural gradients, together with suitable landscape metrics, may

96 favor the quantification of urban forest landscape features and their associations with forest

97 ecological processes (Liu et al., 2009; Ren et al., 2013) and provide possible strategies for forest

98 city design during the fast urbanization process in China (Zhang et al., 2017b).

99   Harbin, a typical provincial capital city in Northeastern China, has been checked for

100 urbanization effects on urban tree species diversity and possible associations with bird species

101 alternations (Xiao et al., 2016a), tree species configuration problems in urban afforestation (Xiao

102 et al., 2016b), and best tree species for improving urban forest soils (Lu et al., 2016; Wang et al.,

103 2017) and soil glomalin and mycorrhizal features (Zhong et al., 2016; Cui & Mu, 2016). However,

104 whole carbon storage at city scale, especially soil organic carbon (SOC), and the relationships with

105 landscape pattern characteristics are still unknown (Ying et al., 2009; Lv et al., 2016).

106   In this paper, we used Harbin, the northernmost province capital city in China, as an example

107 and hypothesized that urban forests have largely different landscape metrics on the basis of the

108 forest type, administrative district, and urban–rural gradients, and these differences are closely

109 associated with forest carbon sequestration in the biomass and soils. The following questions have

110 been answered in this paper: (1) How large are the variations in the characteristics of urban forest

111 landscapes in Harbin City? What are the differences in forest types, administrative districts, and

112 urban–rural gradients? (2) How large are the differences in urban forest biomass and underground

113 soils? Which landscape metrics are most significantly associated with these carbon sequestration

114 differences? (3) Is there any management suggestions from the view of landscape configurations

115 for promoting carbon storage in urban forests? What type of landscape-related suggestions for the

116 exact evaluation of urban forest carbon storage could be derived? The solutions will favor

117 landscape-carbon sequestration sciences and help to define a suitable strategy for urban

118 afforestation and management.

119 **Materials & Methods**

120 **Study area**

121   The study area is located in the urban area of Harbin City (45°45′ N, 126°38′ E; Figure 1), the

122 capital of Heilongjiang Province in Northeastern China. The average elevation of Harbin City is

123 151 m above sea level. The municipal district covers an area of 10,198 km^2. The total area within

124 the fourth ring road is about 600 km^2, and the built-up area within the fourth ring road is 345.3

125 km^2. Until 2014, 4.7 million people lived in the downtown area, according to the Statistical

126 Yearbook of Harbin (http://www.harbin.gov.cn/col/col39/index.html). The mean temperatures in

127 January and July are -17.6 °C (0.3 °F) and 23.1 °C (73.6 °F), according to the climate data from

128 1981 to 2010 (http://data.cma.cn/site/index.html). The annual precipitation is 524 mm (20.6 in).

129   The frost-free period lasts 140 days, while the ice period lasts 190 days (Zhang et al., 2011). The

130   most prevalent soil across Harbin is the black soil (Luvic Phaeozem, FAO) (Chang, 2015).

131   The main region in Harbin City is composed of 5 administrative districts. The main forest

132   types are roadside forest (RF), ecological public welfare forest (EF), landscape and relaxation

133   forest (LF), and affiliated forest (AF), according their location, ecological function, and

134   management objectives (He et al., 2004). Long-term records (up to 1900s) on the urbanization

135   process in Harbin are available. The urban land in Harbin was only 12 km^2 in 1907, and it had

136   increased ca. 30-fold to 333 km^2 in 2014 (Fig. 1). The urban population in Harbin increased 18-

137   fold from 0.54 million in 1946 to 9.87 million in 2014 (Yi et al., 2006). The expansion of ring

138   roads is also a good substitute for urban–rural gradients in Harbin (Huang et al., 2010). These

139   features made Harbin City a good example for the study of urbanization effects on urban forest

140   landscape characteristics and their associations with carbon storage capacity.

141   **Image processing and tree coverage interpretation**

142   Two multispectral GF-1 images with a resolution of 2 m × 2 m (China Center for Resources

143   Satellite Data and Application; CRESDA) acquired on September 26, 2014, were used for the

144   forest coverage extraction. Image preprocessing procedures included radiometric correction,

145   FLAASH atmospheric correction, ortho-rectification, and image fusion and clipping. We extracted

146   the urban forest coverage by using the object-oriented based classification method, according to

147   texture information, spectral information, and spatial attributes of remote sensing images. The

148   attribute assignment and manual modifications were performed with ArcGIS map (ESRI, version

149   10.0).

150   We used per pixel (Wentz & Zhao, 2015) and object-based (Li et al., 2015) validation methods

151   to evaluate the accuracy of urban forest tree coverage extraction. Per pixel methods are used to

152   check whether an individual pixel is classified correctly (Wentz & Zhao, 2015). The overall

153   accuracy of the tree coverage extraction was 97.67%, with a miss factor of 0.06 and detection rate

154   and quality percentage of 94.21%. Object-based accuracy assessment was performed using

155   manually digitalized results from Google Earth satellite images (resolution, 0.59 m) as reference

156   data (Li et al., 2015). We randomly selected 100 plots (500 m × 500 m) to compare the

157   discrepancies between the classified results and reference maps. Figure 2 shows the scatter plot of

158   tree coverage between classification results and corresponding reference data (Google Earth

159   image). It is evident that these scattered points are distributed near the 45° line and R^2 is more than

160   0.99. The results for forest tree coverage in Harbin City are presented in Figure 3.

161   **Analysis of landscape metrics**

162   The analysis of forest landscape characteristics was based on 4 forest types (He et al., 2004),

163   5 administrative districts, 4 ring roads, and 7 periods of urban settlements (Chen et al., 2005; Zhang

164   et al., 2015) and performed using Fragstats (v4.2.589; Fig. 3). The landscape metrics were selected

165   according to their ecological meanings and referenced from Liu et al. (2009) and Gao & Yu (2014).

166   Seven indices (Appendix Table 1 in supplemetall files) were finally selected. The area and edge

167   indices were total area (TA), number of patches (NP), largest patch index (LPI), and mean patch

168   area (AREA_MN); shape index was area-weighted perimeter-area ratio (PARA_AM); and

169   aggregation indices were landscape shape index (LSI) and mean Euclidean nearest-neighbor

170   distance (ENN_MN).

171   The relationships between patch perimeter and patch area are the bases for most shape indices,

172   and the Euclidean nearest-neighbor distance (ENN) is the simplest measure of patch context. We

173   also analyzed the frequency distribution of 4 indices at patch level, namely, patch area, patch

174   perimeter, perimeter-area ratio (PARA), and ENN. The spatial scale for analysis was 2 m, the same

175   as the GF-1 image resolution, and the 8-neighbor patch rule was used.

176   **Field study and estimation of carbon storage**

177   The field study was conducted between August and September 2014. During the field study,

178   we recorded the location of each plot (by using GPS), tree species composition, diameter at breast

179   height (DBH; 1.3 m), basal area (1.3 m, at breast height), and height (measured using a Laster tree

180   height meter, Nikon forestry PRO550 Nikon, Japan) of trees with a diameter greater than 1 cm.

181   The soil samples (0–20 cm) were collected at the same time by using a 100 cm^3 cutting ring (4

182   cutting rings per plot; M&Y Instrument Technology Co. Ltd., Shanghai, China). A fixed volume

183   of intact soil (400 cm³) was stored in a cloth soil bag and air-dried in a dry ventilated room to

184   constant weight for laboratory analysis.

185   The sampling plots were allocated according to forest coverage in different forest types,

186   administrative districts, ring roads, and history of urban settlements (Fig. 1). Plot allocation is

187   listed in Table 1. The estimation of total carbon storage was the random sampling statistics of

188   carbon storage density (carbon stocks per tree cover) of different forest types, ring roads,

189   administrative districts, and history of urban settlements (Lv et al., 2016) and their tree coverage

190   area shown in Figure 3.

191        $$\text{Carbon}_{\text{storage}} = \sum_{i=1}^{j} CD_i \times TC_i \quad (1)$$

192   where CD_i is the *ith* carbon storage density of different forest types, ring roads, administrative

193   districts, and history of urban settlements, and TC_i is the *ith* urban forest tree coverage area of these

194   urban forest classifications.

195   The dryweight biomass of the trees was estimated using tree biomass allometric growth

196   equations obtained from published literature and root-to-shoot ratio of 0.26 when below-ground

197   biomass equations were absent (Appendix Table 2 in supplemental files). Total tree dryweight

198   biomass was converted to total stored carbon by multiplying by 0.5. The biomass carbon storage

199   density (kg C·m⁻²) was estimated using total tree biomass carbon in each plot, divided by the plot

200   area.

201   The SOC content was determined using the heated dichromate/titration method (Bao, 2000;

202   Wang et al., 2011). SOC density in each plot was the product of SOC content, soil bulk density,

203   and sampling soil depth (20 cm in this study).

204   **Statistical analysis**

205   The landscape patterns of the urban forests were characterized by the frequency distribution

206   of different metrics of pooled whole-city data. For finding the changes at urban–rural gradients in

207   ring road development and history of urban build-up, linear regression was used for detecting

208   steady changes during urbanization processes.

209   Pearson's correlation, linear and stepwise regression analyses, smoothing analysis, and

210   bivariate normal distribution were performed using SPSS (version 19.0, 2010, IBM, USA) and

211   JMP (SAS, version 10, USA), respectively, to understand the associations between landscape

212   characteristics and carbon stocks. All tables and figures 2, 4, 5 were created with MS Excel 2010

213   (14.0.4760.1000, Microsoft, Redmond, WA, USA); figures 1 and 3 depicted using ArcGIS 10.0;

214   figure 6 depicted using JMP 10.0.

215

216   **Results**

217   **Spatial distribution and patch characteristics of urban forests**

218   The spatial distribution of urban forests in Harbin was highly uneven (Fig. 3). The large

219   patches mainly belonged to LF, and RF was mainly a long rectangular strip. AF was mainly

220   aggregated in the central urban regions, whereas EF was mainly located in the outer rural region

221   of Harbin City (Figs. 1 and 3). With respect to urban–rural gradients, large patches were mainly

222   distributed in the third ring road region, forest patches in the second ring road region were mainly

223   aggregated in the south area, and north regions of the second ring road had little forest cover. The

224   urban forest in the oldest central urban regions was mainly AF. The urban forests in the newest

225   urbanized regions, such as the north side of Songhua River, were mainly EF. In different

226   administrative districts, most patches in Songbei District were aggregated along Songhua River,

227   and most patches in Xiangfang and Daowai Districts were aggregated in the forest botanical garden

228   and Tianhengshan Park. In summary, the forest patches in all administrative districts were

229   aggregated in several separate areas and most areas were treeless.

230   The forest patches in Harbin were highly fragmented. Small patches covering an area of less

231   than 0.5 ha and patches covering an area of 0.5 to 1 ha accounted for 72.6% and 19.4% of all

232   patches, respectively. Large patches covering an area of more than 1 ha accounted for only 8% of

233   all patches (Fig. 4a). The average patch size was 0.31 ha. Patches with a perimeter of <500 m

234   accounted for 80.2% and patches with a perimeter of more than 1000 m accounted for only 6.9%

235   of all patches (Fig. 4b). The average perimeter of the patches was 388 m. Patches with PARA of

236   more than 0.8 and less than 0.01 accounted for only 7.7% of all patches. More than 90% of the

237   patches had PARA of 0.1 to 0.8, of which 42.6% had PARA from 0.2 to 0.4 (Fig. 4c); the average

238   PARA value was 3251. Most patches (59.62%) were less than 32 m away from the nearest

239   neighboring patches, and only less than 1% of the patches were isolated and more than 512 m

240   away from other patches. ENN of the remaining patches ranged from 32 m to 512 m and they

241   accounted for 39.99% of all patches (Fig. 4d); the average ENN value was 43 m.

242   **Urban forest carbon: Forest types, administrative districts, and urban–rural gradients**

243   The total carbon storage in the different forest types was almost equal, ranging from 127 to

244   133 thousand tons (Table 1). The tree carbon storage density was the highest in EF, and soil carbon

245   storage density was the highest in LF.

246   The peak value for total carbon storage was detected in Xiangfang District (219 thousand

247   tons), which was 4.9-fold higher than the lowest value in Daoli District. The peak value for tree

248   biomass carbon density was observed in Xiangfang District (104 tons ha^{-1}), whereas the peak value

249   for soil carbon density was detected in Daoli District (65 tons ha^{-1}; Table 1).

250   With respect to urban–rural changes, a general pattern of linear decrease from the urban center

251   to rural regions was found with respect to soil carbon density, whereas no steady changes in tree

252   biomass carbon density were found (Table 1). Carbon storage in the first and second ring roads

253   accounted only for less than 10% of the total carbon storage in Harbin, and the highest carbon

254   storage was detected in the fourth ring road (262 thousand tons). With respect to different history

255   of urban settlements, the peak value for total carbon storage was in the unsettled region (250

256   thousand tons), which was 28-fold higher than the lowest value in the 100-year history region (9

257   thousand tons). The peak value for tree carbon density was also in the unsettled region, whereas

258   soil carbon density increased along with the history of urban settlements. The peak value for soil

259   carbon density was in the 100-year region (soil carbon density $= 0.15 \times$ (year of settlement history)

260   $+ 50$, $R^2 = 0.70$, $p < 0.05$, according to our previous study [Lv et al., 2016]).

Landscape metrics: Forest types, administrative districts, and urban–rural gradients

AF comprised the largest proportion of all forest types, with a TA of about 2 times that of EF. The TAs of LF and RF were almost equal. LF had a low level of fragmentation, with the largest LPI (3.59%). The patch size (AREA_MN, 1.97 ha) in LF were 5–12-fold and 5–9-fold higher than that in the other forest types, and the lowest PARA_AM (559) and LSI (43.28) in LF were only half of those in the other forest types. EF had the lowest LPI (0.28%) and the highest ENN_MN (68.89 m); AF and RF had a high level of fragmentation, and they had the lowest AREA_MN (0.22 ha) and higher PARA_AM and LSI than the other forest types (Table 2).

The highest TA of urban forests (1309 ha) and NP (4038) in Xiangfang District were 3.6-fold higher than the lowest TA in Daoli District and 2.8-fold higher than the lowest NP in Daowai District. The largest LPI (13.75%) and AREA_MN (0.42 ha) in Songbei District were 4.6-fold higher than the lowest LPI in Daowai District and 1.9-fold higher than the lowest AREA_MN in Nangang District. The peak value of ENN_MN (62.54 m) in Daowai District was 1.6-fold higher than that of the lowest value in Nangang District (38.57 m; Table 2).

The TA of the suburb urban regions (third and fourth ring roads; 3388 ha) was 9-fold higher than that of the central urban regions (first and second ring roads; 359 ha). The mean patch size (<0.16 ha) in the central urban area was half of that in the suburb area, and PARA_AM in the central urban area was higher than that in the suburban regions (Table 2). The dispersion of patches (LSI) linearly decreased from the fourth ring road region to the first ring road region (LSI = -33.587 $\times$ ring road + 170.35, R^2 = 0.93, p = 0.034; Fig. 5A).

The NP and LSI linearly decreased from the 0-year history region (rural region) to the 100-year region (urban center) (LSI = -0.6093 $\times$ history + 95.299, R^2 = 0.7196, p = 0.033; NP = -27.158 $\times$ history + 3150, R^2 = 0.6642, p = 0.048; Figs. 5B and 5C). The younger history regions like the 10-year region had the highest TA (1382 ha), NP (3858), and AREA_MN (0.36 ha), and they were 20-fold and 2.6-fold higher than the lowest TA (69 ha) and AREA_MN (0.14 ha) in the 80-year region and 12-fold higher than the lowest NP (311) in the 100-year region (Table 2).

287 **Associations between forest carbon traits and landscape metrics**

288 As shown in Table 3 and Figure 6, Pearson's correlation analysis, smoothing analysis, and

289 bivariate normal distribution were used to show the associations between the carbon parameters

290 and landscape metrics. The total tree and soil carbon storage values were positively correlated with

291 TA, NP, AREA_MN, and LSI ($p < 0.01$). Of these 4 indices, peak coefficients were found in TA

292 with tree biomass carbon (0.986) and soil carbon (0.806). The biomass and soil carbon density

293 showed different associations with landscape metrics. When the LF data (outside the bivariate

294 normal distribution ellipse) was excluded, the biomass carbon density was positively correlated

295 with AREA_MN ($p < 0.05$, Table 3, Fig. 6), whereas no marked associations were found with the

296 other indices ($p > 0.05$). The soil carbon density was negatively correlated with TA, NP,

297 AREA_MN, and LSI (Table 3, Fig. 6) and positively correlated with LPI ($p < 0.05$, Table 3, Fig.

298 6). The highest association was found with LPI. No marked relationship was found between soil

299 carbon density and PARA_AM ($p > 0.05$, Table 3, Fig. 6).

300 The stepwise regression analysis showed that both tree carbon storage and soil carbon storage

301 were mainly associated with TA, whereas other factors such as ENN-MN and AREA-MN were

302 included in the regression model (Table 4). When the standard coefficients were compared, the

303 contribution of TA to carbon storage was 3.5–8.1-fold higher than that of EN-MN or AREA-MN.

304 The stepwise regression analysis showed that the soil carbon storage density was mainly associated

305 with LSI (soil carbon storage density = -0.158 × LSI + 69.316, r^2 = 0.51, Table 4), whereas tree

306 carbon storage density was associated with LPI (tree carbon storage density = -1.848 × LPI +

307 90.902, r^2 = 0.125, Table 4). These data showed that the carbon density was regulated to a greater

308 extent by patch configuration and aggregation/dispersion than storage (Table 4).

309 **Discussions**

310 By 2050, there will be 6 billion urban dwellers (Mccarthy et al., 2010). Urbanization, together

311 with climate change, has become the biggest environmental problem worldwide, resulting in

312 increased carbon emissions (Maruotti, 2008; Mccarthy et al., 2010) and urban heat island effects

313 (Zhao et al., 2015; Zhao & Wentz, 2016). Urbanization also affects landscape fragmentation and

314 configuration and diversity of forests (Su et al., 2012) and significantly influences the structure,

315 process, and ecological functions of urban vegetation ecosystems (Yin et al., 2009), including

316 carbon storage function (Zhang et al., 2015; Lv et al., 2016). Urban forest landscape changes along

317 urban–rural gradients are not well-defined, although many ecological functions, such as heat

318 island, biodiversity, tree size, and community features, have been discussed (Larondelle & Haase,

319 2013; Lv et al., 2016; Xiao et al., 2016a; Zhang et al., 2017b). Our study has supplemented

320 information on forest landscape metrics and carbon storage in different forest types, administrative

321 districts, and urban–rural gradients (in terms of ring road and settlement history) for better

322 understanding of landscape characteristics under urbanization effects to provide suitable

323 management measures targeted at different regions. The importance of our findings will be

324 discussed below, together with reference comparisons, management suggestions, and future urban

325 forest evaluations.

326 **Landscape fragmentation of urban forests in Harbin City: Quantification and Comparison**

327   On basis of the overall trend for landscape fragmentation worldwide, fragmentation of the

328 urban forest has been observed to be severe (Liu & Zhang, 2012; Gong et al., 2013). We used

329 Harbin City as an example and quantified and compared landscape characteristics of urban forests

330 in cities localized and worldwide. The mean patch size at city scale was 0.31 ha in Harbin, which

331 was 29.8% of the forest patch size in Changchun (Zhang, 2015) and was low when compared with

332 Shenyang (0.22 to 1.04 ha) (Liu et al., 2009). However, patch density (PD) and mean perimeter-

333 area ratio (PARA) in Harbin, which reached up to 3.18 patches ha^{-1} and 3251, respectively, were

334 both more than 3-fold higher than those in Changchun (Zhang, 2015) and high when compared

335 with Shenyang (PD and PARA ranged from 0.99 to 2.87 patches ha^{-1} and 887 to 4109,

336 respectively) (Liu et al., 2009). These landscape characteristics all indicated a much higher

337 fragmentation level of the urban forests in Harbin than in the localized cities in Northeastern China.

338   Worldwide urbanization has resulted in broad forest fragmentation. In Puerto Rico, forests

339 became more fragmented between 1991 and 2000; the mean patch size decreased and edge to area

340 ratio increased, the dynamics of forest fragmentation were synchronized with the urban sprawl,

341   and the peak forest fragmentation shifted towards the rural areas (Gao & Yu, 2014). In Atlanta,

342   Georgia, forests displayed a fragmentation trend from 1974 to 2005, and this fragmentation trend

343   adversely affected habitat integrity (Miller, 2012). The fragmentation trends caused by

344   urbanization have formed the current spatial structure of urban forests in Atlanta, Georgia (Miller,

345   2012), as in the urban forests in Harbin. The dispersion of patches in terms of LSI and number of

346   patches (NP) decreased along the rural–urban gradients (Fig. 5), showing that forests in the rural

347   regions of Harbin were more dispersed and had more patches than those in the central urban

348   regions. Spatial-temporal gradient analysis of urban green spaces in Jinan also showed that the LSI

349   of residential green space decreased along the rural–urban gradients, and together with other

350   indices, affected urbanization (Kong & Nakagoshi, 2006).

351   Urban forest fragmentation was induced and influenced by many factors, such as urban

352   building density (Liu & Zhang, 2012); deforestation and reforestation processes during urban

353   sprawl (Gao & Yu, 2014); socioeconomic factors such as urban structure change, industry-related

354   economic boom, increase in migrant resident population; and increased income of city residents

355   (Gong et al., 2013); economically driven intense anthropogenic activities; and the absence of a

356   sustainable environmental management and conservation strategy (Gounaridis et al., 2014). The

357   fragmented landscape may degrade habitat quality; threaten species richness, abundance, and

358   composition (Iidaand & Nakashizuka, 1995; Liu et al., 2005); and affect phylogenetic diversity

359   (Matos et al., 2016). This may be a huge risk to forest management in cities such as Harbin. Harbin

360   has experienced an exponential economic growth since the 1980s and population boom since the

361   1950s (Xiao et al., 2016a), resulting in insufficient greenery services in urban regions. The largely

362   fragmented forest landscapes and uneven distribution in different regions of Harbin City require

363   new efforts for urban forest protection, new plantation afforestation, and sustainable management

364   activities for maximizing urban forest services.

365   **Landscape metrics responsible for carbon variations and high carbon-oriented**

366   **managements**

367   Urban forests can provide various ecosystem services and values to a city and its residents,

368   like the removal of air pollutants (Livesley et al., 2016), alleviation of the urban heat island effect

369   (Zhao et al., 2018), and reduction and offset of carbon emissions (Jim & Chen, 2009; Nowak et

370   al., 2013). These ecological functions are linked to landscape characteristics based on the common

371   consensus that environmental patterns strongly influence ecological processes (Turner, 1989;

372   Uuemaa et al., 2013). Our findings highlighted that carbon storage function and landscape pattern

373   of urban forests in Harbin are linked and landscape regulation is possible to improve urban

374   vegetation and soil carbon storage. The carbon storage function of urban forests could contribute

375   to the alleviation of climate changes (Nowak et al., 2002) and reduction of the negative effects of

376   fast urbanization (Martin et al., 2015). The increase of carbon storage at individual tree and patch

377   scale is possible through tree health promotion, forest structure adjustment, tree species selection

378   (Nowak et al., 2002), and soil improvement (Jandl et al., 2007). With respect to landscape pattern,

379   it is important to increase carbon storage through landscape regulation, which should be an aspect

380   of promoting forest ecological function in limited urban areas (Ren et al., 2013; Lv et al., 2016).

381   First, carbon storage in the urban forest trees (and soils) was positively correlated with NP and

382   AREA_MN (Table 3, Fig. 6), which was consistent with the results reported by Wang (2012). In

383   a given urban green space, relatively large forest patches with considerable patch numbers are

384   possible for increasing the urban forest carbon storage in the trees and soils. The much closer

385   relationship between tree carbon storage and TA (Table 3, Fig. 6) indicated that an increase in

386   forest cover is the best way to promote carbon storage function, especially in regions with rather

387   low forest coverage. The increase in total forest coverage could also lower the degree of landscape

388   fragmentation (Liu & Zhang, 2012) and enhance the cool island effect of urban forests (Ren et al.,

389   2015).

390   Second, because of limited green spaces in cities, improvement of carbon storage density (tons

391   ha^{-1}) through landscape regulations should be more practical and focus on forest construction,

392   regulation, and functional promotion. For example, we found that the mean patch size and tree

393   carbon storage density were positively correlated and increasing the mean patch size may promote

394   tree carbon density in future landscape designs.

395   Third, LSI and LPI are 2 landscape metrics for carbon-oriented landscape regulation. Our data

396   have shown that LSI and LPI are closely associated with carbon storage at city and plot density

397   levels (Table 3, Fig. 6). LPI is the percentage of the largest patch in the landscape, mainly reflecting

398   configuration. LSI mainly reflects the aggregation/dispersion of patches. Increasing the

399   connectivity and aggregation of patches (decreasing LSI) and improving the promotion of the

400   largest patch in landscape design may favor urban carbon sequestration.

401   Another parameter for facilitating carbon storage is AREA_MN, which was positively

402   correlated with tree biomass carbon storage after the LF data were excluded (Table 3, Fig. 6). In

403   future urban forest management, afforestation activities targeted at different regions are necessary,

404   especially in regions with low AREA_MN such as Nangang District. Even though tree coverage

405   in Harbin is low, together with other green spaces, green coverage in Harbin could reach up to

406   36% of the whole urban landscape (Lv, 2017). Afforestation in existing grassland, wasteland, and

407   illegal construction land that unites small patches into larger and regular-shaped patches would

408   increase the mean patch size and ecological services.

409   China has devoted a large financial budget for the construction of urban forests, and, by 2020,

410   at least 200 cities will build close-to-nature forests based on the unified design between cities and

411   the countryside to achieve the title of "National Forest City" (Forestry, 2016). On the basis of our

412   findings, Harbin City still has a long way to go to be one of the 200 cities. The urban forest trees

413   in Harbin cover only 7% of the urban lands, which is much lower than the lower limits for forest

414   city (build-up region green coverage, 40% at least). In addition, the uneven distribution of urban

415   forests in the different administrative districts and urban–rural gradients may hinder the unified

416   design concept and lead to discrepancies in the ecological functions provided by urban vegetation

417   in different regions. An increase in tree coverage at city scale is necessary to promote the overall

418   ecological benefits of urban forests in Harbin, especially the establishment of a series of country,

419   city, and community parks. These parks could benefit the local people as long as they open a

420   window or door. Specific designs, such as demolition of illegal structures for tree planting,

421   replanting trees in vacant lots that surround by buildings (Bajsanski et al., 2016; Zhao, 2017; Zhao

422   et al., 2017), and implementation of vertical greening on roofs, walls, and bridges, may increase

423   the connectivity of urban forests and have a positive influence on the fragmented landscape (Gao

424   & Yu, 2014). Previous studies have highlighted that urban greening practices should consider the

425   importance of biodiversity conservation (Xiao et al., 2016a), removal of pollutants (Escobedo &

426   Nowak, 2009; Mu et al., 2004), urban microclimate regulations (Wang et al., 2018), urban heat

427   island mitigation (Zhang et al., 2017a), and urban soil improvement (Cui & Mu, 2016; Wang et

428   al., 2017; Zhou et al., 2017). Our findings strongly suggest that urban forest carbon sequestration

429   in both aboveground biomass and belowground soil carbon should be considered for co-

430   improvement of multiple ecological services.

431   **Implications for the urban forest evaluation and uncertainty**

432   The total carbon storage of the urban forest within the forth ring road of Harbin City was 521

433   to 575 thousand tons, of which 302 to 359 thousand tons belongs to tree carbon; this is more than

434   the above 20 thousand tons estimated by Ying et al. (2009). These findings show the large

435   uncertainty in the estimation of urban forest carbon sequestration (Pouyat et al., 2006). Previous

436   studies on the estimation of carbon storage in urban forests always focused on only vegetation

437   biomass carbon and paid less attention to soil carbon (Nowak et al., 2013; Zhang et al., 2015).

438   Urban soils have robust carbon storage capacity, both in the areas covered by green vegetation

439   (Liu et al., 2016) and beneath the impervious surface (Pouyat et al., 2006; Edmondson et al., 2012;

440   Raciti et al., 2012). In the future, belowground soil carbon storage should be analyzed, and both

441   aboveground and belowground carbon inclusion may help in understanding carbon storage

442   capacity of the whole ecosystem.

443   The scaling up of tree biomass carbon storage in cities was based on several methods without

444   considering landscape metrics, such as model-based estimation including UFORE, CITY green, i-

445   TREE, and InVEST (Nowak et al., 2013); remote sensing image-based estimation by using carbon

446   storage per pixel and vegetation index, such as NDVI (Myeong et al., 2006); forest inventory-

447   based estimation (Zhang, 2015); and random sampling statistics for plot carbon storage and tree

448   coverage/forest coverage area at different land uses (Liu & Li, 2012). In this study, forest type,

449   administrative district, ring road, and history-related urban–rural gradients of the urban forests

450   largely differed in carbon density, and approximate scaling-up showed fluctuations in total urban

451   forest carbon storage from 521 to 575 thousand tons (Table 1). The different storage figures were

452   an over-simplified process; it is the product of forest area and corresponding carbon density in tree

453   biomass and soils. Our findings highlight that, besides forest structure data, the comprehensive

454   relationships among landscape metrics, urbanization gradients, and forest types could be included

455   in a more precise evaluation framework. Several aspects should be considered.

456   First, as shown by the stepwise regression model between carbon storage parameters and

457   landscape metrics, the possible landscape metrics suggested are LSI and LPI for carbon density

458   and TA for total carbon storage estimation in tree biomass and soils (Table 4). With respect to

459   biomass carbon storage, the inclusion of ENN_MN could increase the coefficient (r^2) from 0.65

460   (TA only) to 0.71 (TA and ENN_MN), whereas the soil carbon storage model showed that

461   inclusion of AREA_MN increased r^2 from 0.97 to 0.99 (Table 4).

462   Second, urbanization intensity and forest types should be considered in the estimation model.

463   As shown in Table 1, an approximation of total carbon sequestration based on forest types,

464   administrative districts, and urban–rural gradients showed 1.2-fold differences in biomass and 1.1-

465   fold variations in soil (Table 1). Urbanization-induced improvement of soil carbon has been

466   reported. In our previous study, we found that the urbanization process (from rural to urban: fourth

467   ring road to first ring road, 0-year region to 100-year region) led to the accumulation of SOC in

468   Harbin (Lv et al., 2016), and the same findings were reported in Changchun, China (Zhai et al.,

469   2017). The aggregation and shape complexity of patches decreased (in terms of LSI increased)

470   along with the rural-urban gradients (Fig. 5), and the soil carbon storage density was negatively

471   correlated with LSI (Fig. 6). This may possibly provide an explanation for SOC accumulation from

472   the viewpoint of landscape. Small and shape-complex patches dispersed in the rural landscapes

473 formed larger LSI and more easily exchanged substance and energy with the external environment

474 than the big and regular-shaped patches aggregated in the urban landscapes, including

475 carbonaceous compounds, and may contribute to steady and higher carbon storage in central urban

476 forests. In general, urbanization intensity differences and forest type differences are strongly

477 associated with landscape variations in the forest.

478   Third, background urbanization conditions have been proved to be strongly associated with

479 various ecological functions of urban forests, and their contributions to forest carbon sequestration

480 need to be included. Building geography, e.g., street orientation (Sanusi et al., 2016); street canyon

481 features, e.g., building height and distance to measured trees (Coutts et al., 2016; Morakinyo et al.,

482 2017; Rahman et al., 2017); land use configurations (building, street, green space, and water); and

483 impervious surface percentage (Zhang et al., 2017b) have been proven to affect thermal regulation

484 by trees, biodiversity conservation, and forest structural traits. In this paper, no such data are

485 available, and future studies are required.

486   In the future, a well-matched, large dataset including all the above-mentioned parameters

487 (independent of each other) would facilitate the derivation of a feasible method for scaling-up of

488 city-level carbon storage density or total storage estimation. For example, landscape metrics in a

489 fixed-sized area (e.g., 2 km around the field plot) (Zhang et al., 2017b), together with data on tree

490 size and forest community features, soil carbon density and background road features, impervious

491 surface features, as well as urban–rural gradients and forest types, will favor proper model

492 construction for a proper scaling-up method via a statistical method such as the stepwise regression

493 method used in this study (Table 4). This study has provided hints on the possible parameters for

494 future consideration.

495

496 **Conclusions**

497   The landscape of urban forests in Harbin was highly fragmented when compared with other

498 local cities, and the fragmentation was different in different forest types, administrative districts,

499 ring road- and urban history-related urban–rural gradients. The fragmentation of the landscape was

500   strongly associated with carbon storage functions in trees and soils. LSI increased along with the

501   urban–rural gradients, and its positive relationship with SOC indicates that LSI contributes to the

502   underlying mechanism of urbanization-induced carbon accumulation in highly urbanized regions.

503   The relationships between carbon storage and landscape metrics manifested possible ways to

504   improve the urban forest carbon storage, such as improvement of the whole urban carbon storage

505   by increasing the afforested area. An increase in the largest patch percentage and patch aggregation

506   could increase the soil carbon storage per hectare. This study would help to promote carbon-

507   oriented management practices for urban vegetation and exact evaluation of urban forest carbon

508   sequestration by including landscape metrics and urbanization intensities.

509

510   **Acknowledgements:**

511   Thanks are due to Manli Ren and Zhongxue Pei for their help during field survey, and

512   Professor Kaishan Song for his help while image processing.

513

514   **References**

515   Bao S. 2000. Soil Agro-chemistrical Analysis. China Agriculture Press: Beijing, China.

516   Bajsanski I, Stojakovic V, Jovanovic M. 2016. Effect of tree location on mitigating parking lot
517   insolation. *Computers, Environment and Urban Systems*, 56, 59–67. DOI:
518   10.1016/j.compenvurbsys.2015.11.006

519   Chang J. 2015. The study on the investigation of soil in urban green space and effects for the
520   improving in Harbin. Master of Science, Thesis, Northeast Forestry University.

521   Chen TB, Zheng YM, Lei M, Huang ZC, Wu HT, Chen H, Fan KK, Yu K, Wu X and Tian QZ.
522   2005. Assessment of heavy metal pollution in surface soils of urban parks in Beijing, China.
523   *Chemosphere* 60: 542-551. DOI: 10.1016/j.chemosphere.2004.12.072

524   Edmondson JL, Davies ZG, McHugh N, Gaston KJ and Leake JR. 2012. Organic carbon hidden
525   in urban ecosystems. *Scientific Reports* 2. DOI: 10.1038/srep00963.

526   Escobedo, F, Varela S, Zhao M, Wagner JE. and Zipperer W. 2010. Analyzing the efficacy of
527   subtropical urban forests in offsetting carbon emissions from cities. *Environmental Science &*
528   *Policy* 13: 362-372. DOI: 10.1016/j.envsci.2010.03.009
529 Escobedo FJ. and Nowak DJ. 2009. Spatial heterogeneity and air pollution removal by an urban
530 forest. *Landscape and Urban Planning* 90: 102-110. DOI: 10.1016/j.landurbplan.2008.10.021

531 Forestry C. 2016. The guidance of the construction of Forest City releaseed by the State Forestry
532 Administration. Available at http://www.forestry.gov.cn/main/4818/content-907127.html,
533 (accessed 12 Sepetmber 2016)

534 Gao Q and Yu M. 2014. Discerning Fragmentation Dynamics of Tropical Forest and Wetland
535 during Reforestation, Urban Sprawl, and Policy Shifts. *Plos One* 9. DOI:
536 10.1371/journal.pone.0113140

537 Gong C, Yu S, Joesting H, and Chen J. 2013. Determining socioeconomic drivers of urban forest
538 fragmentation with historical remote sensing images. *Landscape and Urban Planning* 117:57-65.
539 DOI: 10.1016/j.landurbplan.2013.04.009

540 Gounaridis D, Zaimes GN, and Koukoulas S. 2014. Quantifying spatio-temporal patterns of forest
541 fragmentation in Hymettus Mountain, Greece. Computers, *Environment and Urban Systems*
542 46:35-44. DOI: 10.1016/j.compenvurbsys.2014.04.003

543 He X, Liu C, Chen W, Guan Z, and Zhao G. 2004. Discussion on urban forest classification.
544 *Chinese Journal of Ecology* 23:175-178+185. DOI: 10.13292/j.1000-4890.2004.0175

545 Huang D, Su Z, Zhang R, and Koh LP. 2010. Degree of urbanization influences the persistence of
546 Dorytomus weevils (Coleoptera: Curculionoidae) in Beijing, China. *Landscape and Urban
547 Planning* 96:163-171. DOI: 10.1016/j.landurbplan.2010.03.004

548 Iida S, and Nakashizuka T. 1995. Forest fragmentation and its effect on species diversity in sub-
549 urban coppice forests in Japan. *Forest Ecology and Management* 73:197-210. DOI: 10.1016/0378-
550 1127(94)03484-E

551 Jandl R, Lindner M, Vesterdal L, Bauwens B, Baritz R, Hagedorn F, Johnson DW, Minkkinen K,
552 and Byrne KA. 2007. How strongly can forest management influence soil carbon sequestration?
553 *Geoderma* 137:253-268. DOI: 10.1016/j.geoderma.2006.09.003

554 Jim CY, and Chen WY. 2009. Ecosystem services and valuation of urban forests in China. *Cities*
555 26:187-194. DOI: 10.1016/j.cities.2009.03.003

556 Jo HK. 2002. Impacts of urban greenspace on offsetting carbon emissions for middle Korea. *J
557 Environ Manage* 64:115-126. DOI: 10.1006/jema.2001.0491

558 Kong F, and Nakagoshi N. 2006. Spatial-temporal gradient analysis of urban green spaces in Jinan,
559 China. *Landscape and Urban Planning* 78:147-164. DOI: 10.1016/j.landurbplan.2005.07.006

560 Larondelle N, and Haase D. 2013. Urban ecosystem services assessment along a rural–urban
561 gradient: a cross-analysis of European cities. *Ecological Indicators* 29:179-190. DOI:
562 10.1016/j.ecolind.2012.12.022

Li, X, Zhang, C, Li, W, Kuzovkina, YA, and Weiner, D 2015. Who lives in greener neighborhoods? the distribution of street greenery and its association with residents' socioeconomic conditions in hartford, connecticut, USA. *Urban Forestry & Urban Greening, 14*(4), 751-759. DOI: 10.1016/j.ufug.2015.07.006

Liu C, Li J, Li X, He X, and Chen W. 2009. Selection of landscaoe pattern metrics for urban forest based on simulated landscapes. *Journal of Applied Ecology* 20:1125-1131.

Liu C, and Li X. 2012. Carbon storage and sequestration by urban forests in Shenyang, China. *Urban Forestry & Urban Greening* 11:121-128. DOI: 10.1016/j.ufug.2011.03.002

Liu C, Li X, and Guo R. 2007. Forest landscape pattern analysis in different districts of Shenyang. *Journal of Liaoning Forestry Science &Technology*:4-6.

Liu C, and Zhang M. 2012. Landscape defragmentation trends of urban forests under different building densities. *Journal of Northwest Forestry University* 27:266-271.

Liu J, Xiao W, Jiang Z, Feng X, and Li X. 2005. A study on the influence of landscape fragmentation on biodiversity. *Forest Research* 18:222-226.

Liu XL, Li T, Zhang SR, Jia YX, Li Y, and Xu XX. 2016. The role of land use, construction and road on terrestrial carbon stocks in a newly urbanized area of western Chengdu, China. *Landscape and Urban Planning* 147:88-95. DOI: 10.1016/j.landurbplan.2015.12.001

Livesley SJ, McPherson GM, and Calfapietra C. 2016. The Urban Forest and Ecosystem Services: Impacts on Urban Water, Heat, and Pollution Cycles at the Tree, Street, and City Scale. *Journal of Environment Quality*, 45(1), 119. DOI: 10.2134/jeq2015.11.0567

Lu J, Shen G, Wang Q, Ren M, Pei Z, Wei C, and Wang W. 2016. Effect of urban tree species on soil physicochemical properties in Harbin, Northeastern China, and afforestation implications. *Bulletin of Botanical Research* 36:549-555. DOI: 10.7525/j.issn.1673-5102.2016.04.010

Lv HL. 2017. Spatial and temporal variations of urban vegetation and soil carbon storage:a case study in Harbin. D. Phil. Thesis, University of Chinese Academy of Sciences.

Lv H, Wang W, He X, Xiao L, Zhou W, and Zhang B. 2016. Quantifying tree and soil carbon stocks in a temperate urban forest in Northeast China. *Forests* 7:200-218. DOI: 10.3390/f7090200

Maruotti, A. 2008. "The impact of urbanization on CO_2 emissions: Evidence from developing countries." *Ecological Economics* 70(7): 1344-1353. DOI:10.1016/j.ecolecon.2011.02.009

Martin de Jong, Simon Joss, Daan Schraven, Changjie Zhan, and Margot Weijnen. 2015. Sustainable–smart–resilient–low carbon–eco–knowledge cities; making sense of a multitude of concepts promoting sustainable urbanization. *Journal of Cleaner production* 109: 25-38. DOI: 10.1016/j.jclepro.2015.02.004

596 Matos FAR, Magnago LFS, Gastauer M, Carreiras J, Simonelli M, Meira‑Neto JAA, and

597 Edwards DP. 2016. Effects of landscape configuration and composition on phylogenetic diversity

598 of trees in a highly fragmented tropical forest. *Journal of Ecology*. 105: 265–276. DOI:

599 10.1111/1365-2745.12661

600 Mccarthy M P, Best M J, Betts R A. 2010. Climate change in cities due to global warming and

601 urban effects. *Geophysical Research Letters* 37(9): 232-256. DOI: 10.1029/2010GL042845

602 Miller MD. 2012. The impacts of Atlanta's urban sprawl on forest cover and fragmentation.

603 *Applied Geography* 34:171-179. DOI: 10.1016/j.apgeog.2011.11.010

604 Nowak DJ, Greenfield EJ, Hoehn RE, and Lapoint E. 2013. Carbon storage and sequestration by

605 trees in urban and community areas of the United States. *Environ Pollut* 178:229-236. DOI:

606 10.1016/j.envpol.2013.03.019

607 Nowak DJ, Stevens JC, Sisinni SM, and Luley CJ. 2002. Effects of urban tree management and

608 species selection on atmospheric carbon dioxide. *Journal of Arboriculture* 28:113-122.

609 Pouyat RV, Yesilonis ID, and Nowak DJ. 2006. Carbon storage by urban soils in the United States.

610 *Journal of Environmental Quality* 35:1566-1575. DOI:10.2134/jeq2005.0215

611 Raciti SM, Hutyra LR, and Finzi AC. 2012. Depleted soil carbon and nitrogen pools beneath

612 impervious surfaces. *Environ Pollut* 164:248-251. DOI: 10.1016/j.envpol.2012.01.046

613 Ren Y, Wei X, Wang D, Luo Y, Song X, Wang Y, Yang Y, and Hua L. 2013. Linking landscape

614 patterns with ecological functions: A case study examining the interaction between landscape

615 heterogeneity and carbon stock of urban forests in Xiamen, China. *Forest Ecology and*

616 *Management* 293:122-131. DOI: 10.1016/j.foreco.2012.12.043

617 Ren Z, Zheng H, He X, Zhang D, and Yu X. 2015. Estimation of the Relationship Between Urban

618 Vegetation Configuration and Land Surface Temperature with Remote Sensing. *Journal of the*

619 *Indian Society of Remote Sensing* 43:89-100. DOI: 10.1007/s12524-014-0373-9

620 Setala H, Viippola V, Rantalainen AL, Pennanen A, and Yli-Pelkonen V. 2013. Does urban

621 vegetation mitigate air pollution in northern conditions? *Environ Pollut* 183:104-112. DOI:

622 10.1016/j.envpol.2012.11.010

623 Su S, Xiao R, Jiang Z, and Zhang Y. 2012. Characterizing landscape pattern and ecosystem service

624 value changes for urbanization impacts at an eco-regional scale. *Applied Geography* 34:295-305.

625 DOI: 10.1016/j.apgeog.2011.12.001

626 Turner MG. 1989. Landscape ecology: the effect of pattern on process. *Annual review of ecology*

627 *and systematic* 20 :171-197.

628   Uuemaa E, Mander Ü, and Marja R. 2013. Trends in the use of landscape spatial metrics as
629   landscape indicators: a review. *Ecological Indicators* 28:100-106. DOI:
630   10.1016/j.ecolind.2012.07.018

631   Wang W, Qiu L, Zu Y, Su D, An J, Wang H, Zheng G, Sun W, and Sun X. 2011. Changes in soil
632   organic carbon, nitrogen, pH and bulk density with the development of larch (Larix gmelinii)
633   plantations in China. *Global Change Biology* 17: 2657-2676. DOI: 10.1111/j.1365-
634   2486.2011.02447.x

635   Wang W, Zu Y, Wang H, Matsuura Y, Sasa K, and Koike T. 2005. Plant biomass and productivity
636   of Larix gmelinii forest ecosystems in Northeast China: intra-and inter-species comparison. Euasia
637   *Journal of Forest Reseach* 8: 21-41.

638   Wentz E A, Zhao Q. 2015. Assessing validation methods for building identification and extraction.
639   In *Urban Remote Sensing Event* (JURSE). IEEE. 1-4. DOI: 10.1109/JURSE.2015.7120453

640   Xiao L, Wang W, He X, Lv H, Wei C, Zhang B, and Zhou W. 2016a. Urban-rural and temporal
641   differences of woody plants and bird species in Harbin city, northeastern China. *Urban Forestry*
642   *& Urban Greening* 20:20-31. DOI: 10.1016/j.ufug.2016.07.013

643   Xiao L, Wang W, Zhang D, He X, Wei C, Lv H, Zhou W, and Zhang B. 2016b. Urban forest tree
644   species composition and arrangement reasonability in Harbin,northeast China. Chinese Journal
645   of Ecology 35:2074-2081. DOI: 10.13292 /j.1000-4890.201608.027

646   Yi Q, Shuai Y, Wang L, Xue L, and Xu P. 2006. Trends and development process of Harbin
647   population. *Journal of Nanjing college for population programme management* 22:5-8.

648   Yin K, Zhao Q, Cui S, Lin T, and Shi L. 2009. Progresses in urban forest and landscape pattern.
649   *Acta Ecologica Sinica* v.29:389-398.

650   Ying T, Li M, and Fan W. 2009. Estimation pf carbon sotrage of urban forests in Harbin. *Journal*
651   *of Northeast Forestry University* 37:33-35.

652   Zhai C, Wang W, He X, Zhou W, Xiao L, Zhang B. 2017. Urbanization drives SOC accumulation,
653   Its temperature stability and turnover in forests, Northeastern China. *Forests,* 8: 130-148. DOI:
654   10.3390/f8040130

655   Zhang D. 2015. Spatial-temporal changes of urban forest structure and carbon storage under rapid
656   urbanization: A case study in Changchun. D. Phil. Thesis, University of Chinese Academy of
657   Sciences.

658   Zhang D, Zheng H, Ren Z, Zhai C, Shen G, Mao Z, Wang P, and He X. 2015. Effects of forest
659   type and urbanization on carbon storage of urban forests in Changchun, Northeast China. *Chinese*
660   *Geographical Science* 25:147-158. DOI: 10.1007/s11769-015-0743-4

661   Zhang X, Chen L, Ji J, Wang J, Wang Y, Guo W, and Lan B. 2011. Climate change and its effect
662   in Harbin from 1881 to 2010. *Journal of Meteorology and Environment* 27:13-20.

663 Zhao M, Kong ZH, Escobedo FJ, and Gao J. 2010. Impacts of urban forests on offsetting carbon
664 emissions from industrial energy use in Hangzhou, China. *J Environ Manage* 91:807-813. DOI:
665 10.1016/j.jenvman.2009.10.010

666 Zhao, Q. 2017. Evaluating the Effectiveness of Tree Locations and Arrangements for Improving
667 Urban Thermal Environment (PhD Thesis). Arizona State University.

668 Zhao Q, Myint SW, Wentz EA, and Fan C. 2015. Rooftop surface temperature analysis in an urban
669 residential environment. *Remote Sensing* 7(9): 12135-12159. DOI: 10.3390/rs70912135

670 Zhao Q and Wentz EA. 2016. A MODIS/ASTER airborne simulator (MASTER) imagery for
671 urban heat island research. *Data* 1(1). DOI: 10.3390/data1010007

672 Zhao Q, Wentz EA, Murray AT. 2017. Tree shade coverage optimization in an urban residential

673 environment. *Building and Environment* 115, 269 – 280. DOI: 10.1016/j.buildenv.2017.01.036

674 Zhao Q, Yang J, Wang ZH, and Wentz E. 2018. Assessing the Cooling Benefits of Tree Shade by
675 an Outdoor Urban Physical Scale Model at Tempe, AZ. *Urban Science*, 2(1), 4. DOI:
676 10.3390/urbansci2010004

677 Zhong Z, Wang W, Zhang W, and Wang Q. 2016. Compositional variation of glomalin-related
678 soil protein in different forest stands and farmland. *Journal of Beijing Forestry University* 38:107-
679 115. DOI: 10.13332/j.1000-1522.20150399

Figure 1

Location of the study area showing Harbin City in northeastern China, and the distribution of sampling plots at different forest type, administrative districts and urban-rural gradients of different ring road and history of urban settlements in Harbin.
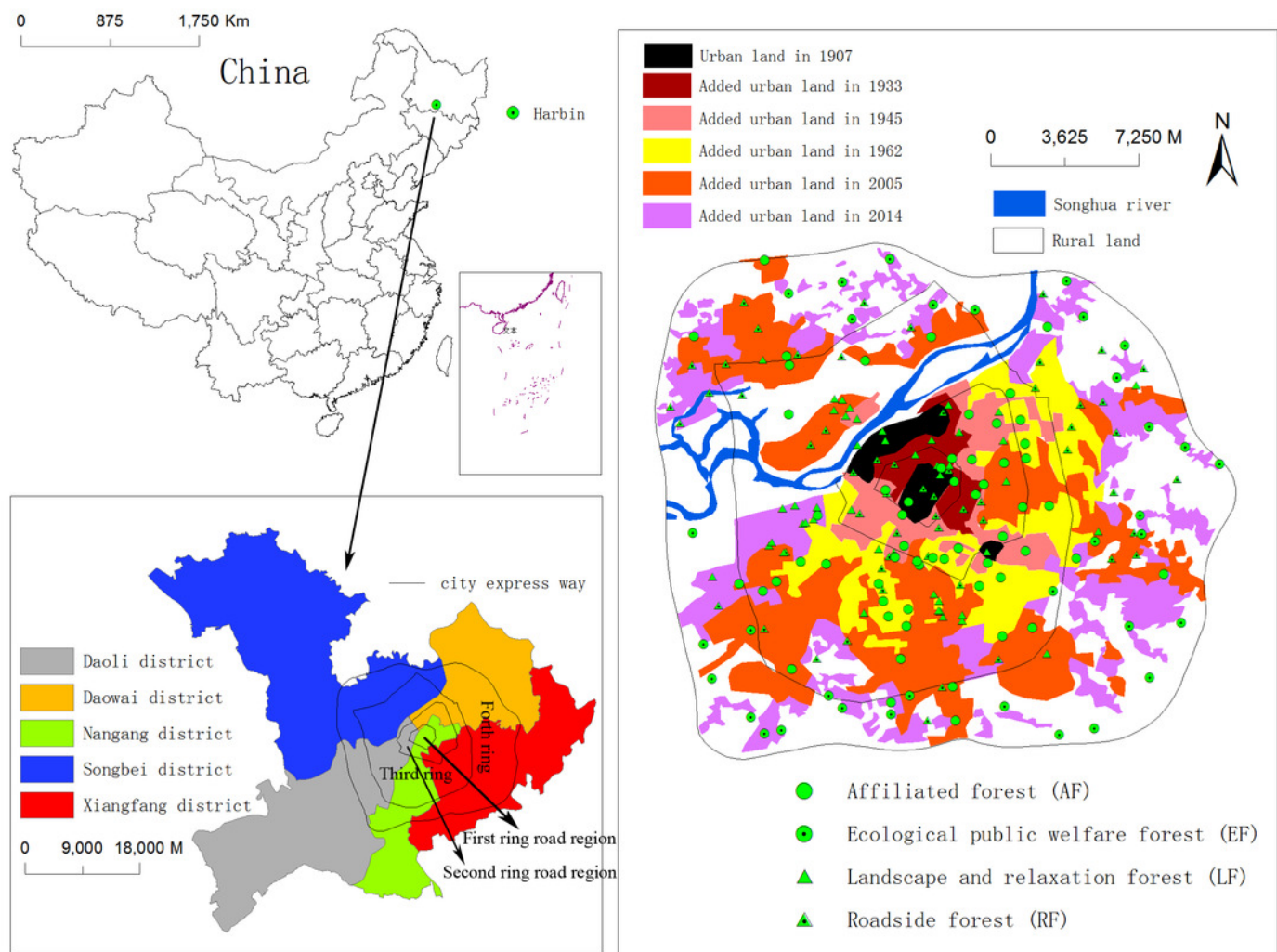
Figure 2

Precision validation for tree cover data of urban forests in Harbin City using Google earth images with a resolution of 0.59 m

$R^2 = 0.9932$

Reference result (m^2) — y-axis

Classification result (m^2) — x-axis
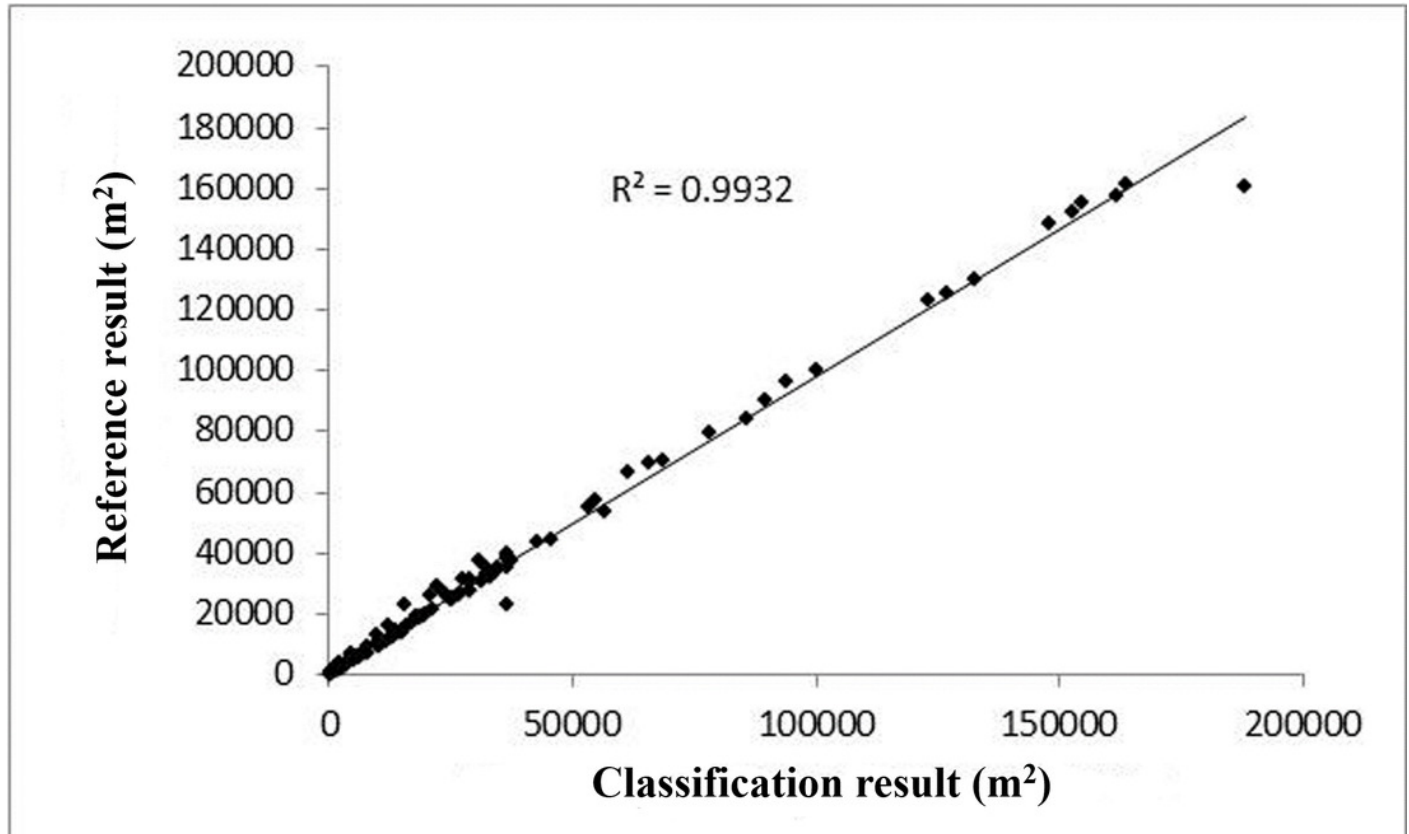
Figure 3

Spatial distribution of urban forests in Harbin City derived from GF1 images (2 m resolution)
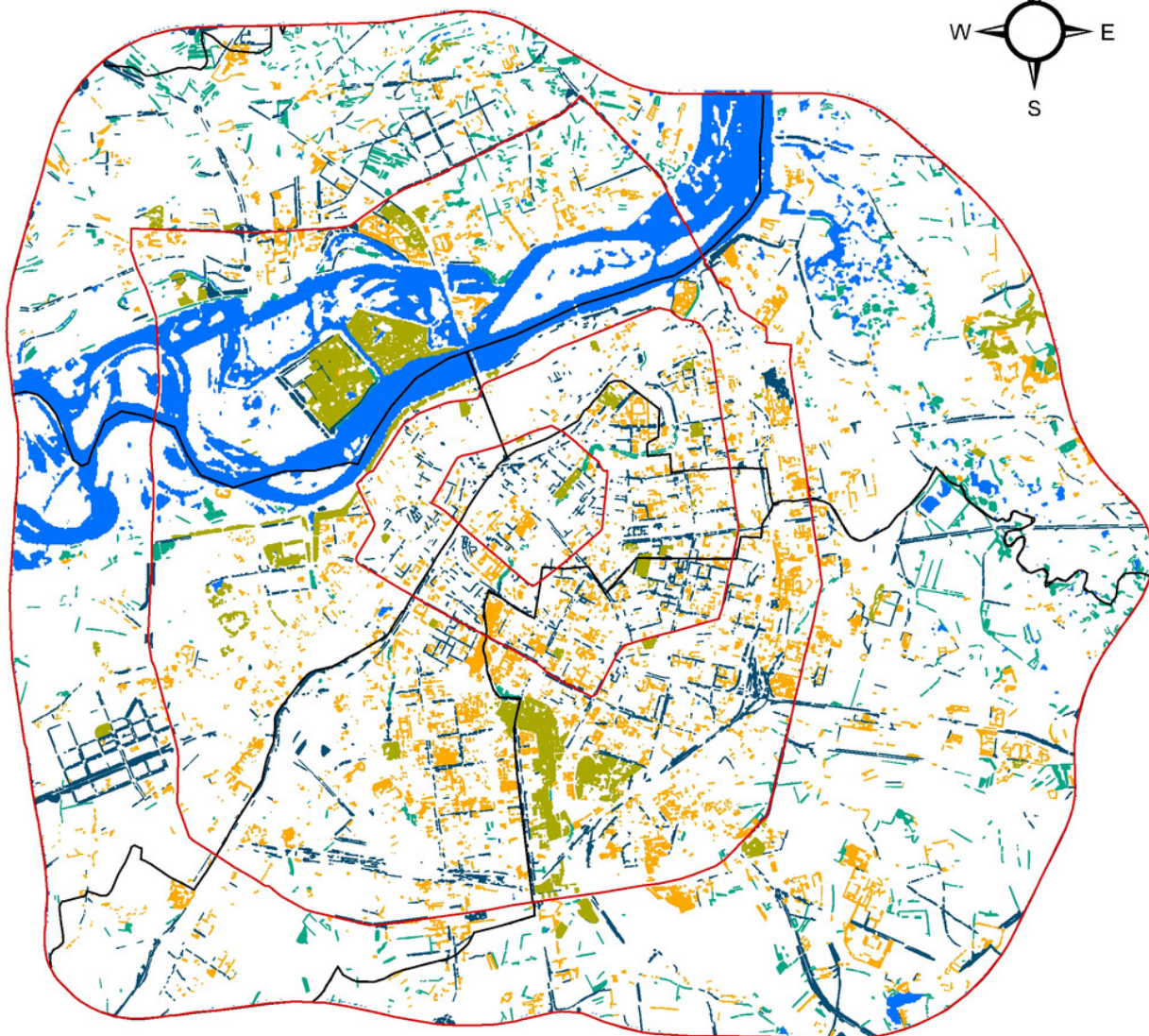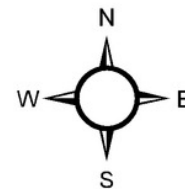
Figure 4

Frequency distribution of urban forests patch area (a), perimeter (b), perimeter-area ratio (c), and Euclidean nearest neighbor distance (d) in Harbin City
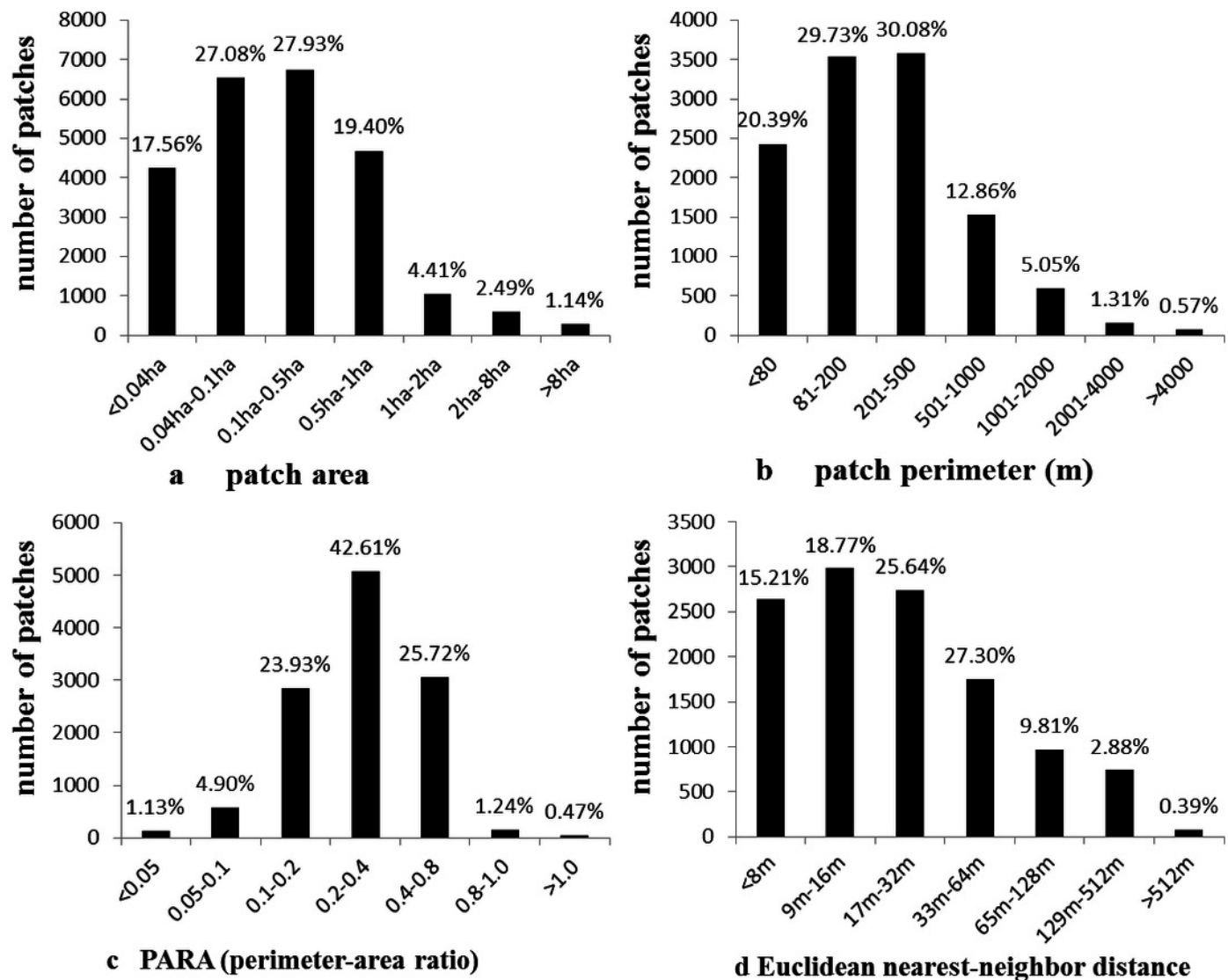
Figure 5

Changes of landscape shape index (LSI) and number of patches (NP) of urban forests along urban-rural gradients (ring roads or history of settlements) in Harbin City.
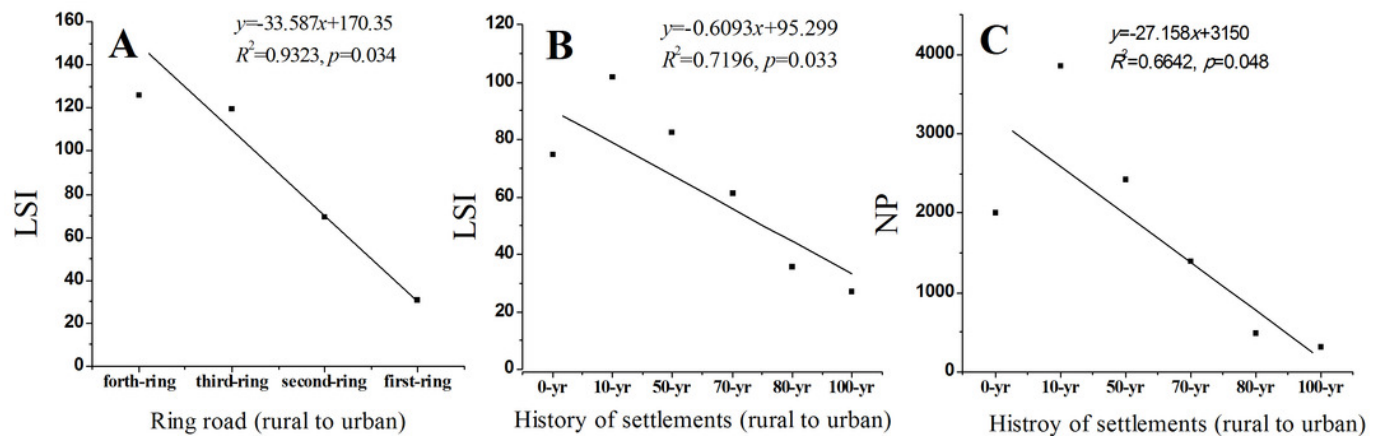
Figure 6

Associations between different landscape metrics and soil-C density, biomass-C density, soil-C storage as well as biomass-C storage.

Note: The line in the figure is the smoothed line of the raw data. The ellipse in the figure is the bivariate normal distribution of the raw data. Triangle is the LF data, which is much larger than other in Area-MN, and without LF, area-MN had good linear relations with various carbon parameters. Different color of the labels in the figures showed the data originated from administrative districts, forest types, urban history and ringroad development regions.
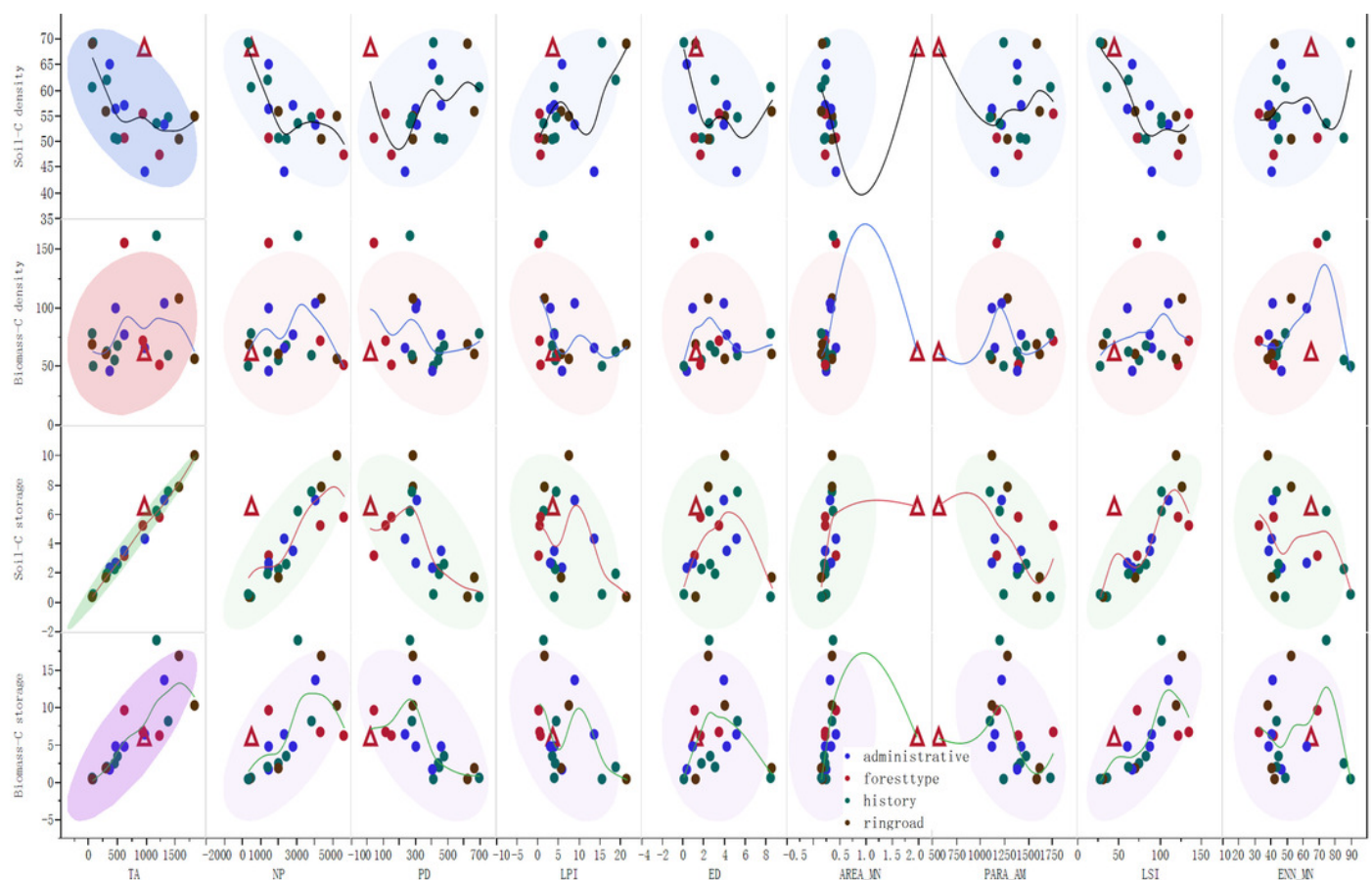
Trees and soils carbon storage for different forest types, administrative districts, urban-rural gradients (ring-roads and history of urban settlements) in Harbin City

Note: AF, affiliated forest; RF, roadside forest; LF, landscape and relaxation forest; EF, ecological public welfare forest. 100-yr, urban area constructed before 1906; 80-yr, urban area constructed between 1933 and 1907; 70-yr, urban area constructed between 1945 and 1934; 50-yr, urban area constructed between 1962 and 1946; 10-yr, urban area constructed between 2005 and 1963; 0-yr, urban area constructed during 2006 and 2014; unsettlement, rural land. The numbers in brackets are standard errors.

1   **Table 1** Trees and soils carbon storage for different forest types, administrative districts, urban-
2   rural gradients (ring-roads and history of urban settlements) in Harbin City

Urban forests classification		No. of plots	Area of the region km²	carbon storage (thousand tons)			C storage density (tons ha⁻¹)	
				Tree	Soil	Total	Tree biomass	Soil
Different forest types and regions								
Forest types	AF	58	12[a]	68.9	63.7	132.6	51.4 (6.4)	47.5 (3.4)
	RF	42	9[a]	72.6	56.2	128.8	71.6 (10.6)	55.4 (3.1)
	LF	62	10[a]	60.9	66.3	127.2	62.9 (8.6)	68.5 (5.5)
	EF	36	6[a]	100.0	32.7	132.7	155.0 (12.2)	50.7 (3.6)
Administrative districts	Daoli	34	90	18.5	26.1	44.6	46.2 (8.3)	65.2 (6.8)
	Daowai	30	96	52.7	29.8	82.5	100.0 (1.9)	56.5 (4.3)
	Nangang	49	92	51.5	38.0	89.5	77.5 (8.3)	57.2 (3.9)
	Songbei	34	143	64.8	43.3	108.1	66.1 (8.4)	44.1 (4.1)
	Xiangfang	50	167	144.8	74.2	219.0	104.0 (13.3)	53.3 (3.4)
Urban-rural gradients								
Ring roads	First ring	16	11	4.8	4.8	9.6	68.8 (13.8)	69.1 (4.9)
	Second ring	32	48	22.7	21.0	43.7	60.8 (8.1)	56.1 (5.7)
	Third ring	77	205	105.1	102.8	207.9	56.1 (5.8)	54.9 (3.4)
	Fourth ring	74	328	178.1	83.4	261.5	108.1 (1.2)	50.6 (3.0)
History of urban settlements	100-yr	7	12	3.8	5.2	9.0	50.3 (16.5)	69.4 (6.3)
	80-yr	10	13	5.4	4.2	9.6	78.7 (15.8)	60.6 (9.0)
	70-yr	28	32	19.7	19.5	39.2	62.6 (9.2)	62.0 (5.1)
	50-yr	27	62	34.8	25.7	60.5	68.4 (14.9)	50.6 (5.2)
	10-yr	44	138	82.4	75.8	158.2	59.6 (9.8)	54.8 (3.3)
	0-yr	51	92	25.0	23.0	48.0	55.2 (8.2)	50.7 (5.0)
	unsettled	32	242	188.0	62.2	250.2	161.8 (13.4)	53.5 (3.9)
Sum		199		302-359	211-219	521-575		

3   Note: AF, affiliated forest; RF, roadside forest; LF, landscape and relaxation forest; EF,
4   ecological public welfare forest. 100-yr, urban area constructed before 1906; 80-yr, urban area
5   constructed between 1933 and 1907; 70-yr, urban area constructed between 1945 and 1934; 50-
6   yr, urban area constructed between 1962 and 1946; 10-yr, urban area constructed between 2005
7   and 1963; 0-yr, urban area constructed during 2006 and 2014; unsettlement, rural land. The
8   numbers in brackets are standard errors. a in superscript is tree coverage area.

Landscape metrics of different types, administrative districts, and urban-rural gradients (ring roads and history of settlements) of urban forests in Harbin City

Note: AF, affiliated forest; RF, roadside forest; LF, landscape and relaxation forest; EF, ecological public welfare forest. 100-yr, urban area constructed before 1906; 80-yr, urban area constructed between 1933 and 1907; 70-yr, urban area constructed between 1945 and 1934; 50-yr, urban area constructed between 1962 and 1946; 10-yr, urban area constructed between 2005 and 1963; 0-yr, urban area constructed during 2006 and 2014; unsettlement, rural land. TA, total area; NP, number of patches; LPI, largest patch index; AREA_MN, mean patch area; PARA_AM, Area mean Perimeter-Area Ratio Distribution; LSI, Landscape Shape Index; ENN_MN, Mean Euclidean Nearest Neighbor Distance Distribution.

1 **Table 2** Landscape metrics of different types, administrative districts, and urban-rural gradients
2 (ring roads and history of settlements) of urban forests in Harbin City

Urban forests classification		TA (ha)	NP	LPI (%)	AREA_MN (ha)	PARA_AM	LSI	ENN_MN (m)
Different forest types and regions								
Forest types	AF	1226	5631	0.69	0.22	1394	121.99	41.63
	RF	942	4327	0.41	0.22	1752	134.38	32.42
	LF	959	488	3.59	1.97	559	43.28	64.57
	EF	620	1463	0.28	0.42	1165	72.47	68.89
Administrative districts	Daoli	364	1477	5.78	0.25	1385	65.98	46.70
	Daowai	474	1435	2.96	0.33	1116	60.70	62.54
	Nangang	614	2803	3.99	0.22	1420	87.67	38.57
	Songbei	981	2315	13.75	0.42	1151	89.74	40.59
	Xiangfang	1309	4038	8.89	0.32	1216	109.62	41.15
Urban-rural gradients								
Ring road regions	First ring	60	372	21.55	0.16	1582	30.55	42.12
	Second ring	299	2001	5.65	0.15	1620	69.65	40.19
	Third ring	1827	5224	7.39	0.35	1121	119.38	38.20
	Fourth ring	1561	4392	1.65	0.36	1278	125.93	52.78
History of urban settlements	100-yr	75	311	15.44	0.24	1242	26.93	89.64
	80-yr	69	482	3.99	0.14	1725	35.67	49.00
	70-yr	315	1404	18.86	0.22	1385	61.27	43.60
	50-yr	508	2418	3.47	0.21	1468	82.57	44.93
	10-yr	1382	3858	4.36	0.36	1100	101.71	43.31
	0-yr	453	2008	4.12	0.23	1407	74.77	85.30
	unsettled	1169	3067	1.44	0.38	1196	102.02	74.16

3 Note: AF, affiliated forest; RF, roadside forest; LF, landscape and relaxation forest; EF,
4 ecological public welfare forest. 100-yr, urban area constructed before 1906; 80-yr, urban area
5 constructed between 1933 and 1907; 70-yr, urban area constructed between 1945 and 1934; 50-
6 yr, urban area constructed between 1962 and 1946; 10-yr, urban area constructed between 2005
7 and 1963; 0-yr, urban area constructed during 2006 and 2014; unsettlement, rural land. TA, total
8 area; NP, number of patches; LPI, largest patch index; AREA_MN, mean patch area;
9 PARA_AM, Area mean Perimeter-Area Ratio Distribution; LSI, Landscape Shape Index;
10 ENN_MN, Mean Euclidean Nearest Neighbor Distribution.

Pearson correlation analysis between landscape metrics and biomass and soil carbon storage (thousand tons) of urban forests in Harbin City. Number of sample size = 20.

Note: * represent 0.05 significant level, and ** represent 0.01 significant level. TA, total area; NP, number of patches; LPI, largest patch index; AREA_MN, mean patch area; PARA_AM, Area mean Perimeter-Area Ratio Distribution; LSI, Landscape Shape Index; ENN_MN, Mean Euclidean Nearest Neighbor Distance Distribution.

1 **Table 3** Pearson correlation analysis between landscape metrics and biomass and soil carbon
2 storage (thousand tons) of urban forests in Harbin City. Number of sample size = 20.

Items	Pearson correlation	TA (ha)	NP	LPI (%)	AREA_ MN (ha)	PARA _AM	LSI	ENN_M N (m)
Storage (ton)	Tree C	**0.986****	**0.782****	-0.388	**0.608****	**-0.505***	**0.769****	-0.238
	Soil C	**0.806****	**0.609****	-0.422	**0.716****	-0.370	**0.687****	0.026
Density (ton ha^{-1})	Tree C	0.196	0.043	-0.353	**0.533***	-0.154	0.180	0.276
	Soil C	**-0.518***	**-0.644****	**0.466***	**-0.503***	-0.060	**-0.713****	0.182

3 Note: * represent 0.05 significant level, and ** represent 0.01 significant level. TA, total area;
4 NP, number of patches; LPI, largest patch index; AREA_MN, mean patch area; PARA_AM,
5 Area mean Perimeter-Area Ratio Distribution; LSI, Landscape Shape Index; ENN_MN, Mean
6 Euclidean Nearest Neighbor Distance Distribution.

Stepwise regression between forest carbon parameters and landscape metrics. Stepwise Criteria: Probability-of-F-to-enter <= 0.200, Probability-of-F-to-remove >= 0.300.

1 Table 4. Stepwise regression between forest carbon parameters and landscape metrics. Stepwise

2 Criteria: Probability-of-F-to-enter <= 0.200, Probability-of-F-to-remove >= 0.300.

Response variables	Parameters	Unstandardized Coeff.		Standardized Coeff.	t-value	Sig.	R²
		B	Std. Error	Beta			
Density							
SOC density	(Constant)	69.316	3.183		21.780	0.000	0.508
	LSI	-0.158	0.037	-0.713	-4.312	0.000	
Biomass-C density	(Constant)	90.092	10.161		8.866	0.000	0.125
	LPI	-1.848	1.153	-0.353	-1.603	0.126	
Storage							
Biomass-C storage	(Constant)	-4.702	2.847		-1.651	0.117	0.708
	TA	0.009	0.001	0.870	6.414	0.000	
	ENN_MN	0.081	0.044	0.249	1.838	0.084	
SOC storage	(Constant)	-0.051	0.150		-0.342	0.736	0.986
	TA	0.005	0.000	0.959	32.050	0.000	
	AREA_MN	0.849	0.215	0.118	3.956	0.001	